

## Chemical bonding in the $\text{UFe}_{1-x}\text{Ni}_x\text{Al}$ alloys

I. M. Reznik

*Physics and Technology Institute of Ukrainian Academy of Sciences, R. Luxembourg Strasse 72, 340114 Donetsk, Ukraine*

F. G. Vagizov

*W. Trzebiatowski Institute of Low Temperature and Structure Research, Polish Academy of Sciences,  
50-950 Wrocław, P.O. Box 937, Poland  
and Physicotechnical Institute, Russian Academy of Sciences, Sybirski Trakt 10/7, 42009 Kazan, Russia*

R. Troć

*W. Trzebiatowski Institute of Low Temperature and Structure Research, Polish Academy of Sciences,  
50-950 Wrocław, P.O. Box 937, Poland*

(Received 17 December 1993; revised manuscript received 29 August 1994)

Chemical bonding in  $\text{UFe}_{1-x}\text{Ni}_x\text{Al}$  is interpreted within the framework of nonempirical calculations of charge-density distribution, performed by means of the modified statistical method. Maps of constant density in the principal planes of the crystal structure are presented. It is shown that an electron-density (ED) distribution exhibits a pronounced charge transfer from the [Al-Fe(Ni)] plane towards the [U-Fe(Ni)] plane as the Ni concentration in the alloy changes up to  $x \approx 0.3$ . As a result of such a transfer, the ED distribution in the latter plane becomes largely nonuniform. Chemical bonding within the [Al-Fe(Ni)] group of ions shows mostly a covalent character. Thus, such regions determine, to a large extent, the electric-field gradient at the  $^{57}\text{Fe}$  nuclei. Results of theoretical investigations of chemical bonding peculiarities in the  $\text{UFe}_{1-x}\text{Ni}_x\text{Al}$  alloys are compared with Mössbauer-effect data. On this basis we have attempted to explain the anomalous behavior of the lattice parameters in the solid solutions  $\text{UFe}_{1-x}\text{Ni}_x\text{Al}$ .

### I. INTRODUCTION

The uranium ternary compounds (UTM) containing a transition metal ( $T$ ) and a main-group element ( $M$ ) encompass a large class of intermetallics, exhibiting unusual physical properties, particularly a variety of magnetic behavior. The reason for this lies in the peculiarities of interactions of  $5f$  electrons with the ligand electrons. In particular, the anisotropic hybridization between these electrons acting in a similar way to a crystal-field effect<sup>1</sup> may play an important role.

However, the occurrence of a large family of  $\text{UT}_x\text{M}_y$  intermetallics also gives evidence about the unique character of chemical bonding in these phases. Without knowledge of the latter it is rather difficult to understand sufficiently clearly the observed nature of their magnetic behavior.

The basic understanding of the modern theory of chemical bonding is the knowledge of the charge- and spin-density distribution in the unit cell.<sup>2</sup> Their fundamental role is the basis of functional theory.<sup>3</sup> According to this work, the electron-density (ED) distribution determines the properties of the ground state of a crystal. This distribution also illustrates all the peculiarities in chemical bonding, clearly emphasizing the general characteristics of interionic interactions.

The ED distribution of all electrons can be observed by x-ray-scattering experiments. However, the problem of resolving small changes in the valence ED from the total density is beyond experimental accuracy in these interme-

tallic compounds. As many examples have shown,<sup>2</sup> a lot of information can be obtained by means of *ab initio* calculations. Some chemical bonding characteristics obtained in this way can be confirmed experimentally and supply a fundamental ground for their proper interpretation. One such experiment is the quadrupolar splitting (QS) of a Mössbauer spectrum line, being proportional to the electric-field gradient (EFG) at a Mössbauer nucleus.

Solid solutions like  $\text{UFe}_{1-x}\text{Ni}_x\text{Al}$  can be regarded as a representative example in the family of  $\text{UT}_x\text{M}_y$  ternary compounds. The above alloys present a series of anomalies in their physical properties, especially those connected with a significant deviation from Vegard's law and a nonlinear dependence of the quadrupolar splitting on the composition.<sup>4,5</sup>

In the present work, we report the results of theoretical ED calculations performed for the  $\text{UFe}_{1-x}\text{Ni}_x\text{Al}$  alloys and we compare the results obtained with the Mössbauer data.<sup>4,5</sup> This allows us to draw important conclusions about the peculiarities of chemical bonding in these uranium ternary intermetallics.

### II. BASIC THEORETICAL ASSUMPTIONS

The problem of determining the ED distribution in a crystal is traditionally closely connected with the solution of a one-electron problem within the local-density approximation.<sup>6</sup> In the past ten years, first of all due to the development of the linear muffin-tin orbital (LMTO) method,<sup>7</sup> self-consistent solutions became possible for

crystals containing several tens of electrons in the unit cell (see, for example, Ref. 8). However, these calculations remain complicated since the solutions of a secular problem of high dimension must be solved for a large number of points in the Brillouin zone. There is a possibility to avoid these difficulties using a simplified theory in which the interelectronic potential is directly connected to the ED distribution.

Such a connection can be obtained in the framework of simplified approximations of the nonuniform electron gas. There are well-known cases of such approximations. In the case of a weak potential, it is possible to use a perturbation theory (PT), which well describes the ground-state properties of simple metals. However, PT fails in the case of semiconductors, dielectrics, and transition metals. The second way of ED calculations is a quasi-classical approximation, that is better known as the statistical method or Thomas-Fermi approach (TFA). The criterion of its applicability is that the potential changes are very slow.<sup>9</sup> Of course, it is also exact in the long-wavelength limit. Less obviously, as some practical calculations have shown, this method reflects with high accuracy the response of the electron subsystem in semiconductors to the self-consistent potential.<sup>10</sup> In the latter case, this potential cannot be regarded as being small, but only a few components of its Fourier series expansion play a decisive role. The error increases with the appearance of the meaningful short-wave part of the potential expansion. In such a case, a significant improvement can be achieved in a theory in which the potential is represented as the sum of two components. One of them is smooth, but with varying amplitude, while the second is small, but can rapidly fluctuate.

Such a theory has been presented in a previous work,<sup>11</sup> and its general form is given in Ref. 12. Here we will give only those formulas that are important to understanding the scheme of the present calculations.

Let us consider the Dirac density matrix  $\gamma(\bar{r}\bar{r}'\varepsilon)$  and its related Green function  $\Gamma(\bar{r},\bar{r}',\varepsilon)$ :<sup>13</sup>

$$\gamma(\bar{r},\bar{r}',\varepsilon) = -\frac{1}{\pi} \text{Im} \int_{-\infty}^{\varepsilon} \Gamma(\bar{r},\bar{r}',\varepsilon) d\varepsilon, \quad (1)$$

where Im denotes the imaginary part. The electron density is the diagonal element of  $\gamma(\bar{r},\bar{r}',\varepsilon)$ .

In the case of free electrons  $V(\bar{r})=0$ , and

$$\Gamma(\bar{r},\bar{r}',\varepsilon) = \Gamma_0(\bar{r},\bar{r}',\varepsilon) = -\exp(ikR)/2\pi R \quad (3),$$

where  $R = |\bar{r} - \bar{r}'|$  and  $k^2 = 2\varepsilon$ . In the general case

$$\Gamma(\bar{r},\bar{r}',\varepsilon) = \Gamma_0(\bar{r},\bar{r}',\varepsilon) + \int \Gamma_0(\bar{r},\bar{r}'',\varepsilon) V(\bar{r}'') \Gamma(\bar{r}'',\bar{r}',\varepsilon) d\bar{r}'' \quad (2)$$

If we rewrite this equation in the form

$$\begin{aligned} & \Gamma(\bar{r},\bar{r}',\varepsilon) - \Gamma_0(\bar{r},\bar{r}',\varepsilon) \\ &= U(\bar{r}) \int d\bar{r}'' \Gamma_0(\bar{r},\bar{r}'',\varepsilon) \Gamma(\bar{r}'',\bar{r}',\varepsilon) \\ &+ \int d\bar{r}'' \Gamma_0(\bar{r},\bar{r}'',\varepsilon) \Gamma(\bar{r}'',\bar{r}',\varepsilon) [V(\bar{r}'') - U(\bar{r})], \end{aligned} \quad (3)$$

where  $U(\bar{r})$  is an arbitrary function, and assume that  $U(\bar{r})$  is such a function that the second integral on the right-hand side of Eq. (3) can be considered as a small perturbation, then the solution can be formally written down up to any order:

$$\Gamma(\bar{r},\bar{r}',\varepsilon) = \sum_{j=0}^{\infty} \Gamma_j(\bar{r},\bar{r}',\varepsilon). \quad (4)$$

According to Eq. (1) we get the corresponding expression for  $\gamma(\bar{r},\bar{r}'\varepsilon)$  with

$$\begin{aligned} \gamma_j(\bar{r},\bar{r}',\varepsilon) &= \frac{\tilde{k}(\bar{r}')}{2\pi^2} \theta(\tilde{k}(\bar{r}')^2) \\ &\times \int_j \cdots \int_{j_1} \left[ \tilde{k}(\bar{r}') \sum_{l=1}^{j+1} S_l \right] S_{j+1}^{-1} \\ &\times \prod_{l=1}^j \left[ -\frac{dr_l}{2\pi S_l} [V(\bar{r}_l) - U(\bar{r})] \right], \end{aligned} \quad (5)$$

where  $j_1$  is the spherical Bessel function,  $S_l = |\bar{r}_l - \bar{r}_{l-1}|$ ,  $\bar{r}_{j+1} = \bar{r}'$ ,  $\bar{r}_0 = \bar{r}$ ,  $\theta(x) = 1$  if  $x > 0$  and if  $x < 0$ , and

$$\tilde{k}^2(\bar{r}) = k^2 - 2U(\bar{r}) = 2[\varepsilon - U(\bar{r})]. \quad (6)$$

The expression (5) resembles a form of perturbation theory for  $\gamma$  suggested by March, Young, and Sampanthar.<sup>13</sup> There are two distinctions between them. First, the formula (5) includes local momentum  $\tilde{k}(\bar{r}')$  defined by the expression (6), instead of the constant Fermi momentum  $k$ . Secondly, we have  $V(\bar{r}_l) - U(\bar{r})$  instead of  $V(\bar{r}_l)$ . Therefore the present theory may be considered as a re-ordered perturbation theory in which the zeroth-order term yields the Thomas-Fermi ED for potential  $U(\bar{r})$ . Using the possibility of free choice for  $U(\bar{r})$ , in particular, we may put  $U(\bar{r}) = V(\bar{r})$  to obtain the original TFA in zero order or  $U(\bar{r}) = 0$  for the standard perturbation theory.

For actual numerical applications it is most efficient to restrict the TFA series to the first order, preserving in expression (4) the terms with  $j=0,1$  only. Then we get

$$\begin{aligned} \rho(\bar{r}) &= \frac{\tilde{k}(\bar{r})^3}{6\pi^2} - \frac{\tilde{k}(\bar{r})^2}{4\pi^3} \int \frac{j_1(2\tilde{k}(\bar{r})|\bar{r} - \bar{r}'|)}{|\bar{r} - \bar{r}'|^2} \\ &\times [V(\bar{r}') - U(\bar{r})] d\bar{r}' \end{aligned} \quad (7)$$

if  $\varepsilon > U(\bar{r})$  and  $\rho(\bar{r}) = 0$ . The zeroth order of this expression coincides with the one that describes the electron density of an electron gas in the field  $U(\bar{r})$  in the TFA.

In Ref. 11 the following expression has been proposed for  $U(\bar{r})$ :

$$U(\bar{r}) = \frac{\tilde{k}}{2\pi} \int \frac{j_1(2\tilde{k}|\bar{r} - \bar{r}'|)}{|\bar{r} - \bar{r}'|^2} V(\bar{r}') d\bar{r}'. \quad (8)$$

If  $U(\bar{r})$  satisfies this equation exactly then the second term in Eq. (7) disappears. This complicated integral equation for  $U(\bar{r})$  simplifies greatly if we take an average value  $\langle k \rangle$  instead of  $\tilde{k}$  in the right-hand side of Eq. (8) and preserve the second term in Eq. (7).

We know that

$$V(\vec{r}) = V_{ps}(\vec{r}) + \int \rho(\vec{r}') / |\vec{r} - \vec{r}'| d\vec{r}' + V_{xc}(\rho(\vec{r})), \quad (9)$$

where  $V_{ps}(\vec{r})$  is the ion-core potential, the integral defines the Coulomb and  $V_{xc}(\vec{r})$  is the exchange-correlation potential. The formulas (7), (8), and (9) correspond to a first order TFA and allow one to find the ED with the help of a proper self-consistent procedure.<sup>12</sup>

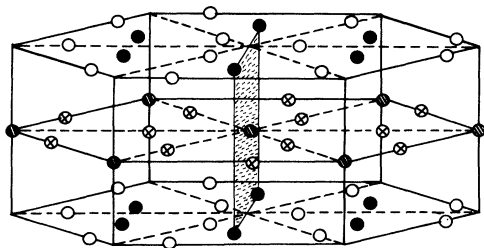
In all expressions mentioned above we suppose that the electron states are singly occupied. For the case of closed shells, where for every orbital both spin directions are possible, the expressions (5) and (7) must be doubled.

We apply this method to the analysis of chemical bonding as well as to the quadrupole interactions in uranium intermetallic compounds, namely, to the case of  $UFe_{1-x}Ni_xAl$  solid solutions.

### III. GENERAL DATA

It is well known<sup>14-16</sup> that these compounds crystallize in a hexagonal structure of  $HoNiAl$  type (space group  $P62m$ ) with three formula units per unit cell (see Ref. 4). This structure is schematically shown in Fig. 1. The U and Al atoms occupy the positions (3g) and (3f), respectively, while the transition-metal (here Fe and Ni) atoms are distributed in the (1b) and (2c) sites, forming two basic atomic planes, i.e., the (U-Fe) and (Al-Fe) planes, with different local environments.

These differences are reflected in  $^{57}Fe$  Mössbauer spectra in the different intensities of Mössbauer lines, as well as in their splittings due to quadrupolar interactions (Fig. 2). In Ref. 5 it was pointed out that the substitution of Fe by Ni atoms causes a nonmonotonic change of quadrupole splitting which implies different probabilities of Ni-atom distribution at the (1b) and (2c) sites in the crystal unit cell (Fig. 3). A similar behavior is observed in the concentration dependence of lattice parameters  $a$  and  $c$  (Fig. 4), giving rise to an important deviation from Vegard's law. As is the case of  $\Delta_{QS}(x)$ , the lattice parameters  $a$  and  $c$  below and above  $x \sim 0.3$  follow a straight-line dependence, but at  $x \sim 0.3$  a discontinuity in slope occurs with a maximum for the  $a$  axis and a minimum for



Iron or Nickel	●	1b	$(0, 0, 1/2)$
	●	2c	$\pm(1/3, 2/3, 0)$
Aluminium	○	3f	$(y, 0, 0), (0, y, 0), (\bar{y}, \bar{y}, 0)$
Uranium	⊗	3g	$(x, 0, 1/2), (0, x, 1/2), (\bar{x}, \bar{x}, 1/2)$

FIG. 1. Crystal structure of the  $Fe_2P$  ( $HoNiAl$ ) type. The marked Fe-Fe plane, drawn perpendicularly to the basal atomic layers, is used in the analysis (see text).

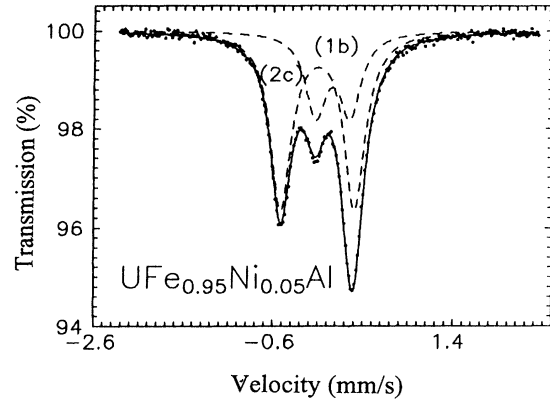


FIG. 2.  $^{57}Fe$  Mössbauer spectra for  $UFe_{0.95}Ni_{0.05}Al$ , consisting of two different quadrupole splittings associated with the crystallographic positions (1b) and (2c) (dashed lines).

the  $c$  axis (Fig. 4). Nevertheless, we think that the sharp break in  $\Delta_{QS}(x)$  observed at the same composition is not directly connected with the respective dependence of the lattice parameters, although the latter dependence should somehow influence the magnitudes of the QS. It seems that the main reason is the change in the electron-density

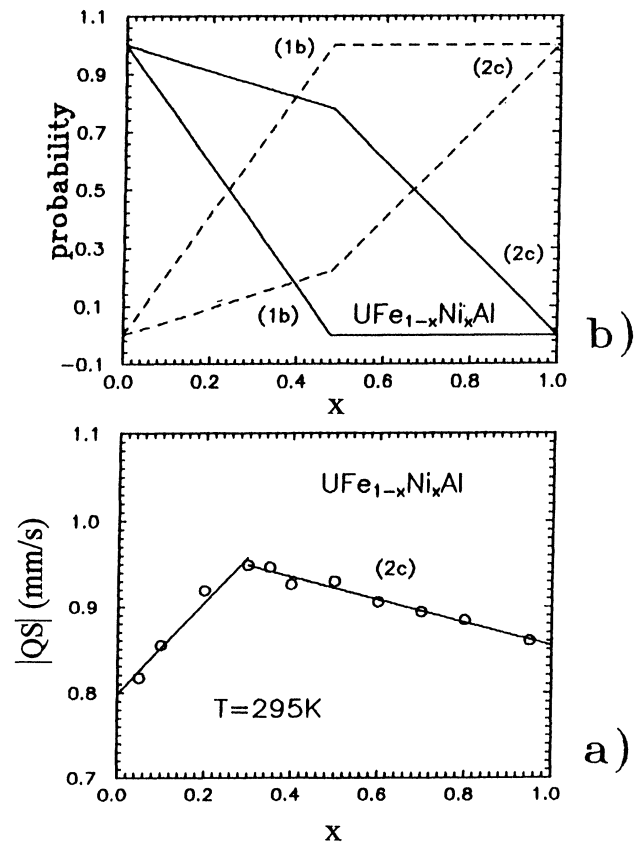


FIG. 3. Mössbauer data for  $UFe_{1-x}Ni_xAl$ : (a) Quadrupole splitting of Fe atoms at the (2c) positions, and (b) occupancy probability of the crystallographic sites (1b) and (2c) by Ni atoms depending on the composition  $x$ .

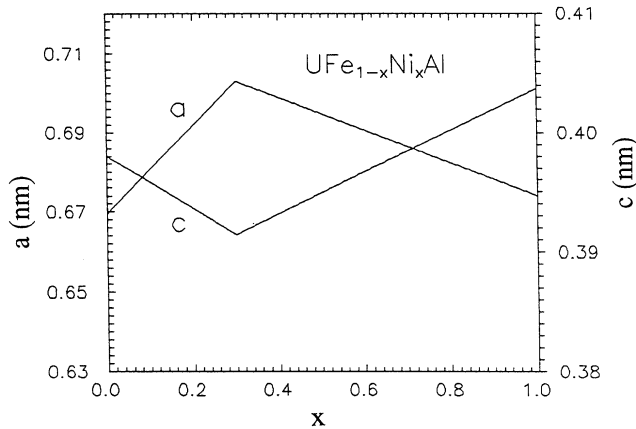


FIG. 4. Schematic change of the lattice parameters  $a$  and  $c$  for  $\text{UFe}_{1-x}\text{Ni}_x\text{Al}$  as a function of Ni concentration.

distribution around the respective atomic sites (see Ref. 17).

An analysis of the area under the resonance curve (Fig. 2) leads to the conclusion that with increasing  $x$  the Fe atoms are first substituted by Ni at the (1b) position (U-Fe plane). Consequently the Mössbauer spectra allowed us to estimate the probability that Ni substitutes at the (1b) or (2c) sites in the process of exchanging with the Fe atoms.

Although the lattice parameter of the  $\text{UFeAl}$  unit cell can be regarded as well determined, neither the accurate positions nor the distribution of U and Al atoms in the unit cell are well known. For example, in the paper by Dwight *et al.*<sup>16</sup> the values  $x_{\text{U}}=0.58$  and  $y_{\text{Al}}=0.25$  are given for the internal parameters of the isostructural compound  $\text{HoNiAl}$ , while slightly different values of  $y_{\text{Al}}$  are reported in other literature (see, e.g., Ref. 18).

Thus, with the exception of some internal parameters (positions of the U and Al atoms in the unit cell), we have enough crystallographic data to perform nonempirical

calculations for the  $\text{UFe}_{1-x}\text{Ni}_x\text{Al}$  alloys. The deviation from stoichiometry of the alloys with  $0 < x < 1$  is described within a virtual-crystal method: the pseudopotential of each lattice site is treated as a weighted average of ionic potentials, where the weight is taken equal to the probability of a site occupation by the relevant ion.

There is another nontrivial problem, namely, about the choice of ionic pseudopotentials for U, Fe, and Ni which is discussed below. Similar to previous work,<sup>17</sup> we use for the ions of metals the well-known simple form<sup>19</sup> of the potential, namely,

$$V_{ps}^i(r) = -Z^i / \max(R^i, r). \quad (10)$$

This contains two parameters: the core charge  $Z^i$  and its radius  $R^i$ . This expression is of course very simplified for describing the peculiarities of one-electron spectra, but for the valence ED distribution it is quite adequate. It allows us to reveal with enough accuracy the differences in the sizes of atoms as well as in the charges of cores. For Fe, Ni, and Al we take  $Z^i=3$ , while for U  $Z^{\text{U}}=4$ . The values of  $Z$  are connected to the valence or, qualitatively, to the number of electrons which change their states considerably by forming chemical bonding. In this meaning, it is preferable to use values of  $Z$  which are as large as possible, for example,  $Z=6$  for U. But in such a case the potential becomes deeper and its Fourier expansion becomes more slowly convergent. Our calculations show that for  $Z^{\text{U}}=6$  the distribution of two additional electrons is nearly spherically symmetric around the nucleus. Therefore the results obtained for the EFG and conclusions about chemical bonding are practically the same as for  $Z^{\text{U}}=4$ , but for the latter case the Fourier convergence is much better.

In order to determine the parameters  $R^i$  we applied the following procedure. Using the data of Ref. 20, we find the differences between the x-ray-scattering amplitudes of atoms and their  $Z$ -charged ions. These differences may be expressed by the Fourier transform of the valence electron densities. Furthermore, we computed valence ED's for the U, Fe, Ni, and Al atoms using potentials of the

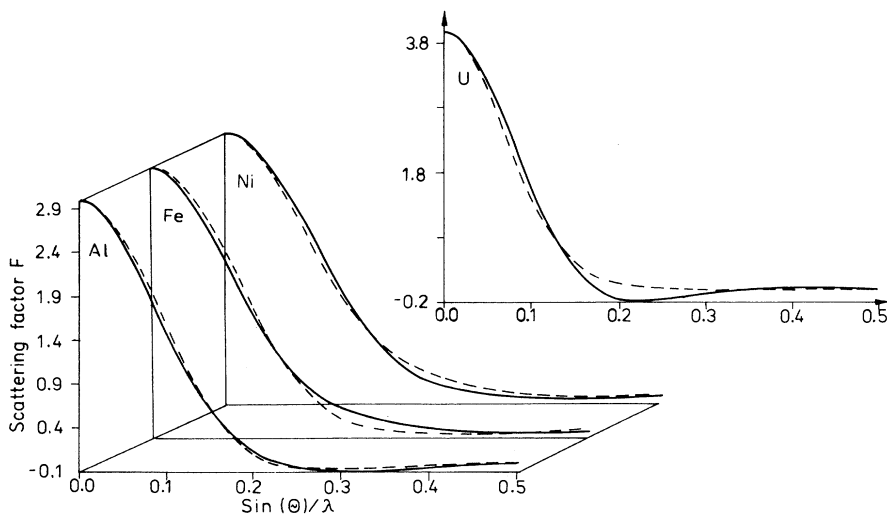


FIG. 5. Valence electron scattering factors for Al, Fe, Ni, and U as a function of  $\sin\theta/\lambda$ . The full lines represent those taken from the Ref. 20, while the dashed lines represent the fitted values.

form (10) with the theory described above. Then we fit the  $R^i$  values to achieve the minimum deviation between the scattering factors calculated in this manner and their tabulated values. We have obtained the following values:  $R^{\text{Fe}}=2.0$ ,  $R^{\text{Ni}}=1.90$ ,  $R^{\text{Al}}=2.2$ , and  $R^{\text{U}}=2.8$  a.u. The results of this procedure are shown in Fig. 5. It allows us to draw a conclusion about the accuracy of the described theory in the case of isolated atoms. If one uses a more complex form of the potential than Eq. (10) and the same procedure for finding its parameters, then the above fit may be improved considerably. However, our attempts in this direction did not qualitatively change the main results that we will describe below.

#### IV. RESULTS

##### A. Stoichiometric $\text{UFeAl}$ : The peculiarities of its chemical bonding

Valence charge-density maps in the basal (Al-Fe) plane as well as in the parallel (U-Fe) plane, obtained as a result of self-consistent calculations for  $y_{\text{Al}}=0.30$ , are shown in Fig. 6. The following observations can be made.

(1) The valence ED distribution in the (U-Fe) plane is relatively uniform (the amplitude of the ED varies by about 30% around the average value). Strong covalent interactions are certainly absent. The chemical bonding in this plane has clear metallic character.

(2) In the basal (Al-Fe) plane (the variation of the ED is about 70% around its average value), the maxima of valence ED charge are distributed along the directions between nearest-neighbor Al-Fe atoms, with a corresponding bond charge. Therefore the chemical bonding in this plane can be characterized by a large homopolar component. Hence we conclude that substitution of Fe by Ni atoms will give a larger gain for the (1*b*) positions. This conclusion is fully confirmed by Mössbauer experiment.<sup>4,5</sup>

Despite these qualitative conclusions the charge distributions obtained allowed us to calculate the EFG at the Fe nuclei, which can be derived from the obtained QS of Mössbauer lines. For this purpose we use the Fourier expansion of  $\rho(\vec{r})$  in terms of reciprocal lattice vector  $\vec{G}$  and use the formula for the EFG

$$V_{ij}(\vec{r}) = 4\pi \sum \rho_{\vec{G}} \bar{G}_i \bar{G}_j / \bar{G}^2 \exp(i\vec{G}\vec{r}). \quad (11)$$

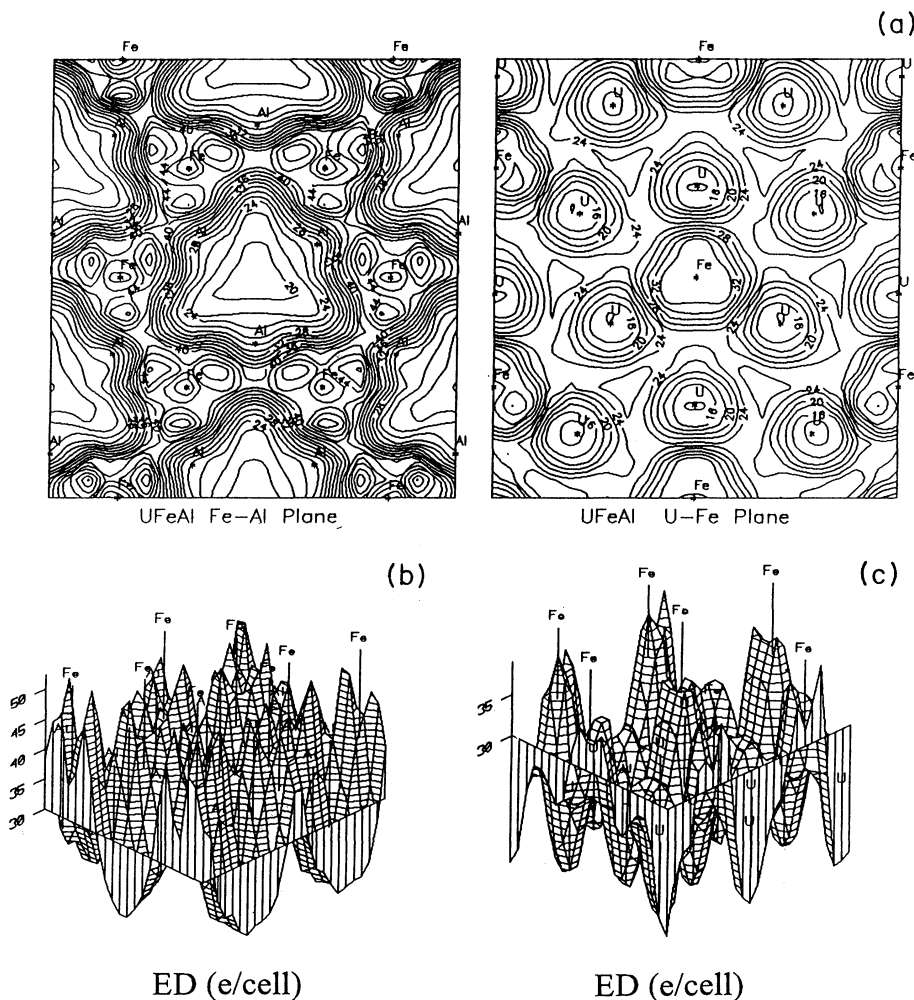


FIG. 6. (a) Contour plots of the electron-density distribution in two types of crystallographic planes of  $\text{UFeAl}$ , and (b) and (c) three-dimensional electron-density distribution.

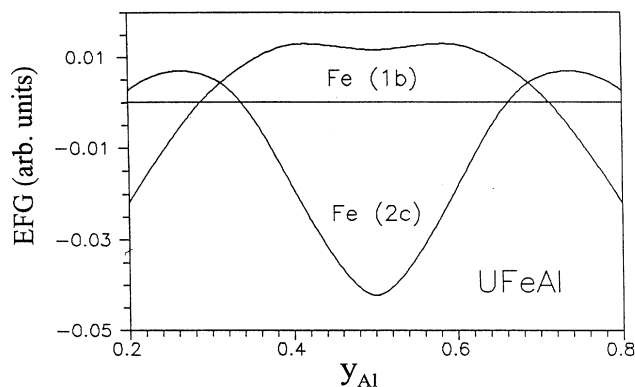


FIG. 7. Calculated electric-field gradient (EFG) at the Fe site for UFeAl as a function of the parameter  $y_{Al}$ .

The component connected with the field of ionic cores (lattice part) was found by the Ewald method.<sup>21</sup> The main eigenvalues obtained by diagonalization of the tensor  $V_{ij}(\bar{r})$ , named  $V_{zz}$ , in dependence on the position of Al ( $y_{Al}$ ), are shown in Fig. 7. The magnitude of the QS being proportional to  $V_{zz}$  is given by the expression<sup>22</sup>

$$\Delta E_Q = e^2 \sqrt{(1 + \eta^2/3)} Q (1 - \gamma_\infty) V_{zz} / 2. \quad (12)$$

Here  $Q$  is the quadrupole moment of the nucleus,  $\gamma_\infty$  the Sternheimer antishielding factor, and  $\eta$  the asymmetry

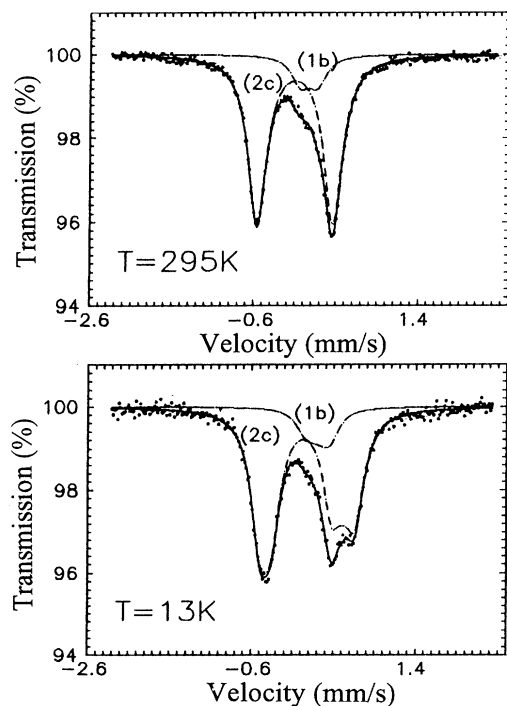


FIG. 8. Room-temperature and 13 K  $^{57}\text{Fe}$  Mössbauer spectra for  $\text{UFe}_{0.5}\text{Ni}_{0.5}\text{Al}$ . The dashed lines for the 13 K spectrum clearly show that the sign of the QS for the (1b) and (2c) sites of Fe atoms is opposite. The RT spectrum is shown for comparison.

parameter. Since the value of the term  $Q(1 - \gamma_\infty)$  is not known with sufficient accuracy, we will concentrate on relative data. For example, the experimental  $|\Delta_{QS}|$  value of  $^{57}\text{Fe}$  Mössbauer spectra for UFeAl at position (2c) is twice that at position (1b). From Fig. 7 it is clear that in the reasonable range of  $y_{Al}$  values this ratio of 2 occurs around  $y_{Al} \sim 0.27, 0.30,$  and  $0.42$ . For a choice of the most proper value of  $y_{Al}$  it is worthwhile to draw attention to the sign of the EFG at different crystallographic sites and on the direction of the main axis of the EFG tensor in relation to the easy direction of magnetization. From Mössbauer experiments on  $\text{UFe}_{0.5}\text{Ni}_{0.5}\text{Al}$  at temperatures where it is magnetically ordered (Fig. 8) we note that the best fitting of spectra can be achieved if one assumes the  $V_{zz}$  has different signs at the (1b) and (2c) sites. This in turn allows us to conclude that the most consistent EFG values are obtained for either  $y_{Al} \approx 0.27$  or  $0.42$ .

### B. Solid solutions $\text{UFe}_{1-x}\text{Ni}_x\text{Al}$

An analysis of the area under resonance curves of Mössbauer spectra, obtained for  $\text{UFe}_{1-x}\text{Ni}_x\text{Al}$  (Fig. 3),<sup>5</sup>

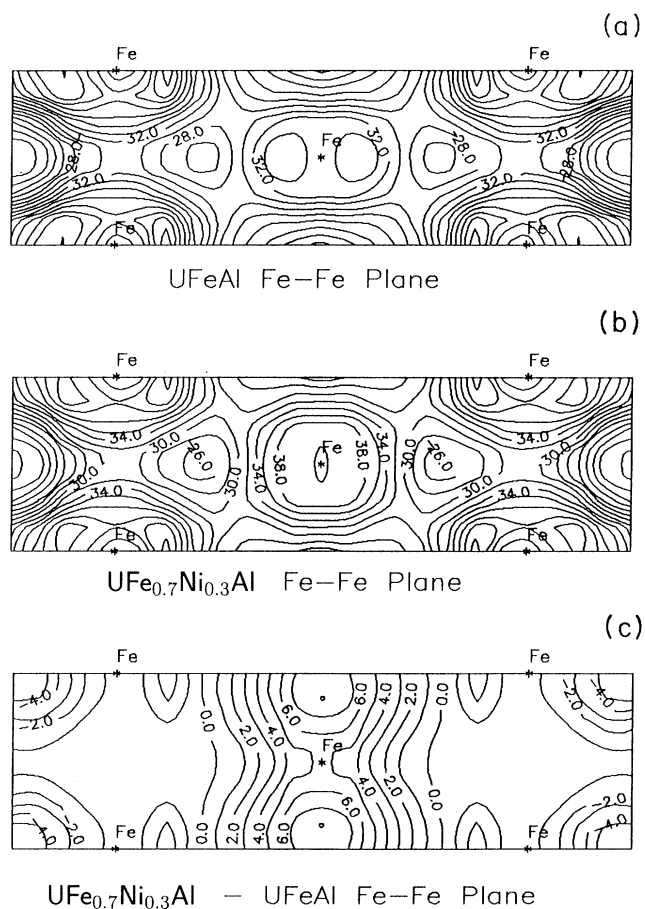


FIG. 9. Two-dimensional maps of the electron-density (ED) distribution in the (Fe-Fe) plane especially chosen (see Fig. 1). They are shown for two cases, (a)  $\text{UFeAl}$  and (b)  $\text{UFe}_{0.7}\text{Ni}_{0.3}\text{Al}$ , while (c) gives the difference in the ED distribution between these two alloys. Note the differential ED at the (1b) positions.

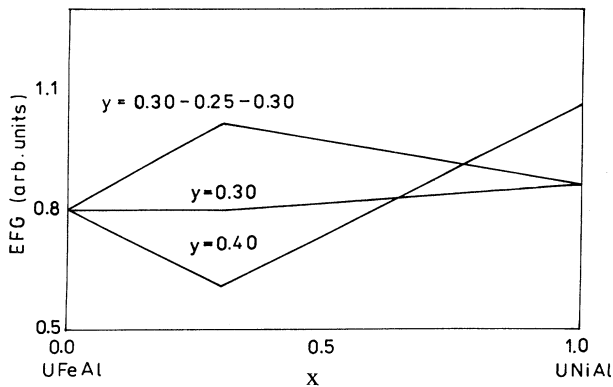


FIG. 10. Calculated EFG as a function of  $x$  assuming different values of  $y_{\text{Al}}$ . Compare this figure with Fig. 3(a), where the experimental QS versus  $x$  curve for Fe at the (2c) site is presented for  $\text{UF}_{e_{1-x}\text{Ni}_x\text{Al}}$  solid solutions.

indicates that for  $x \leq \frac{1}{3}$  Ni exchanges for the Fe ions first of all at the (1b) sites. In fact, the calculations of the valence charge distribution have been shown that the Fe atoms have a considerably stronger bond at (2c) than at (1b). Therefore the Ni atoms would favor the (1b) sites.

The model pseudopotential of Ni can be regarded as being “deeper” than that of the Fe atom. This simply reflects that Ni has a smaller ionic (atomic) radius and is also slightly more electronegative than Fe. Therefore the occurrence of the Ni atoms at the (1b) positions not only increases the ED by introducing additional valence electrons but also leads to a charge transfer from the basal plane towards the U-Fe(Ni) plane (Fig. 9). In consequence of this transfer both planes attract each other more strongly, diminishing considerably the parameter  $c$ . This process continues until all the (1b) positions are fully occupied by Ni ions, i.e., at  $x = \frac{1}{3}$ . For higher substitution, Ni can only exchange for Fe at the (2c) sites, transferring charge again into the [Al-Fe(Ni)] plane, and thus make the distribution of electrons in the unit cell more uniform. This weakening of the attraction between the planes causes the parameter  $c$  to increase while the parameter  $a$  decreases.

We have made calculations of the EFG, depending on the Ni concentration, using the values of occupation numbers from experiment<sup>5</sup> [see Fig. 3(b)]. The results of these calculations are shown in Fig. 10, where with  $y_{\text{Al}} = 0.3$  or 0.4 the EFG (taken as the QS) for UFeAl and UNiAl agrees qualitatively with experiment (one should remember that we compare the relative variables). However, the dependence of quadrupolar splitting on the con-

centration  $x$  is in contrast to the Mössbauer data [compare Fig. 3(a)]. It appears that the absolute value of the EFG at the Fe(2c) site is nearly constant ( $y = 0.3$ ) or diminished ( $y = 0.4$ ) when  $x$  increases up to  $\frac{1}{3}$ , in contradiction with Mössbauer measurements. We suppose that this discrepancy is caused by neglecting the changes in the internal parameters of the U and especially the Al atoms as a function of  $x$ . If we assume that  $y_{\text{Al}}$  changes linearly from 0.30 to 0.25 (and from 0.25 to 0.30) in the subinterval of  $0 \leq x \leq 0.33$  ( $0.33 \leq x \leq 1.0$ ), qualitatively good agreement with experiment (see Fig. 10) is achieved.

## V. CONCLUSIONS

The comparison of the theoretical results with the Mössbauer experimental data allows one to draw the following conclusions.

(1) The valence charge distribution in the [Al-Fe(2c)] basal plane is nonuniform to a large extent and the chemical bonding between Al and Fe can be characterized by a large covalent component, while chemical bonding between U and Fe in the [U-Fe(1b)] plane is mainly of metallic character.

(2) The difference in the ED distribution gives evidence that the Fe atoms are more strongly bound in the basal (Al-Fe) plane than those in the (U-Fe) plane. Therefore, Ni in the  $\text{UF}_{e_{1-x}\text{Ni}_x\text{Al}}$  alloys substitutes first for Fe at the (1b) sites.

(3) The exchange of the Fe atom at the (1b) sites by Ni causes a polarization of the electron cloud from the basal (Al-Fe) plane towards the [U-Fe(Ni)] plane. In consequence, a stronger attraction between the crystallographic layers occurs which leads to a decrease in the lattice parameter  $c$  and simultaneously to an increase in  $a$ . On the contrary, the occupancy of the (2c) positions ( $x > \frac{1}{3}$ ) by Ni raises the  $c$  value due to the subsequent reduction of the polarization mentioned above.

(4) The free parameter of the Al atoms,  $y_{\text{Al}}$ , is assumed to change slightly when the  $c$  ( $a$ ) parameter changes.

(5) The concentration dependence of the quadrupole splitting (or EFG) is first of all influenced by the probability of the occupancy of (1b) and (2c) sites by Fe (Ni) in the unit cell and to some extent by the variation in the lattice parameters.

## ACKNOWLEDGMENTS

We would like to thank Professor B. Ya. Sucharevski for his interest in this work. We also thank Professor H. Stachowiak and Professor J. Mulak for critical reading of the manuscript. The work was supported by Grant No. 202969101 of the State Council for Scientific Research.

<sup>1</sup>B. Johansson, O. Eriksson, L. Nordstrom, L. Severin, and M. S. S. Brooks, *Physica B* **172**, 101 (1991).

<sup>2</sup>V. G. Tsirelson, I. M. Reznik, and R. P. Ozerov, *Crystallogr. Rev.* **3**, 11 (1992).

<sup>3</sup>P. Hohenberg and W. Kohn, *Phys. Rev.* **136**, B864 (1964).

<sup>4</sup>R. Troć, V. H. Tran, F. G. Vagizov, H. Drulis, *J. Alloys Compounds* **200**, 37 (1993).

<sup>5</sup>R. Troć, V. H. Tran, F. G. Vagizov, and H. Drulis, preceding paper, *Phys. Rev. B* **51**, 3003 (1995).

<sup>6</sup>W. Kohn and L. J. Sham, *Phys. Rev.* **4**, 1133 (1965).

- <sup>7</sup>H. L. Skriver, *The LMTO Method*, Springer Series in Solid State Science Vol. 41 (Springer, Berlin, 1984), p. 1.
- <sup>8</sup>B. Johansson, O. Eriksson, L. Nordstrom, M. S. S. Brooks, and H. L. Skriver, *Physica B* **144**, 32 (1986); *Phys. Scr.* **T13**, 65 (1986).
- <sup>9</sup>W. Harrison, *Pseudopotentials in the Theory of Metals* (W. A. Benjamin, New York, 1966).
- <sup>10</sup>A. Balderschi, K. Mashke, A. Milchev, and R. Pickenhain, *Phys. Status Solidi B* **108**, 511 (1981).
- <sup>11</sup>I. M. Reznik, *Fiz. Tverd. Tela (Leningrad)* **30**, 3496 (1988) [*Sov. Phys. Solid State* **30**, 2009 (1988)].
- <sup>12</sup>I. M. Reznik, *Electron Density Distribution in the Theory of Ground State Properties of Solids* (Naukova Dumka, Kiev, 1993), p. 175 (in Russian); *Prog. High Temp. Supercond.* **32**, 3297 (1992).
- <sup>13</sup>N. H. March, W. H. Young, and S. Sampanthar, *The Many Body Problem in Quantum Mechanics* (Cambridge University Press, Cambridge, England, 1967).
- <sup>14</sup>D. J. Lam, J. B. Darby, Jr., J. W. Downey, and L. J. Norton, *J. Nucl. Mater.* **22**, 22 (1967).
- <sup>15</sup>C. W. Kimbal, R. H. Hannon, C. M. Hummel, A. E. Dwight, and G. K. Shenoy, *Rare Earth and Actinides* (Institute of Physics, London, 1971), p. 105.
- <sup>16</sup>A. E. Dwight, M. H. Mueller, R. A. Conner, Jr., J. W. Downey, and H. Knot, *Trans. Metall. Soc. AIME* **242**, 2075 (1968).
- <sup>17</sup>V. V. Bakenko, V. G. Bootko, A. A. Gusev, and I. M. Reznik, *Sverkhprovodimost* **3**, 22 (1990).
- <sup>18</sup>D. J. Lam, J. D. Darby, Jr., and M. V. Nevitt, in *The Actinides: Electronic Structure and Related Properties*, edited by A. J. Freeman and J. B. Darby (Academic, New York, 1974), Vol. 2, p. 175.
- <sup>19</sup>M. L. Cohen, V. Heine, and D. Weaire, in *Solid State Physics: Advances in Research and Applications*, edited by H. Ehrenreich, F. Seitz, and D. Turnbull (Academic, New York, 1970), Vol. 24, p. 1.
- <sup>20</sup>Don T. Cromer and J. T. Waber, in *International Tables for X-ray Crystallography*, edited by J. A. Ibers and W. C. Hamilton (Kynoch, Birmingham, 1974), Vol. 4, p. 71.
- <sup>21</sup>J. M. Ziman, *Principles of the Theory of Solids* (Cambridge University Press, London, England, 1964), p. 360.
- <sup>22</sup>*Chemical Applications of Mössbauer Spectroscopy*, edited by V. I. Goldanskii and R. H. Herber (Academic, New York, 1968), p. 701.